

LOW-CYCLE FATIGUE PROPERTY AND LIFE PREDICTION MODEL OF TC18 TITANIUM ALLOY MATERIAL

SU Shaopu, WANG Binwen, CHEN Xianmin, LI Lei and DONG Dengke

¹ National Key Laboratory of Strength and Structural Integrity, Aircraft Strength
Research Institute of China, Xi'an, Shaanxi, 710065, China

Abstract: The static and low-cycle fatigue behaviors of TC18 titanium alloy were investigated through the strain-controlled fatigue tests, such as the stress-strain constitutive relationship, the cyclic stress-strain curve and the strain-life curve. In order to meet the requirements of engineering fatigue life evaluation for TC18, based on Manson-Coffin and reliability analysis theory, the fatigue life model was built for strain-controlled tests, and the low-cycle fatigue life curve was observed to investigate the life, fractography results indicated that the fracture profiles of static sample and fatigue sample had different crack initiation locations and fracture characterizations; on the other hand, combined with the damage mechanical theory, the gradual degradation process of the mechanical properties of TC18 titanium alloy with the increase of load cycles was described by the Lemaitre ductile damage model, and the fatigue damage accumulation parameters were determined based on experimental results.

Keywords: TC18 Titanium alloy, low-cycle fatigue life, damage evolution, Lemaitre ductile damage model

INTRODUCTION

As a highly alloyed near- β type titanium alloy, TC18 titanium alloy is widely applied in the landing gear and flap slides with the advantages of high strength, excellent plasticity and weldability [1-2]. Yet more aircraft service datum show that low-cycle fatigue failure sometimes occurs in the arresting hook of carrier-based aircraft due to its serious servicing environment. The structures, such as arresting hook and ejection rod, would be repeatedly impacted with high load when the aircraft is landing, thus the damage of this parts is initiated at low-cycle fatigue lives. Consequently, the research on low-cycle fatigue performance plays an important role in the fatigue life evaluation of aircraft load-bearing structural parts.

Most of researchers focus on the microscopy characteristics, static strength and stress-based fatigue life prediction of TC18 in view of experimental results, and its constitutive models have been obtained based on the softening mechanisms, yet the studies on elastic-plastic damage life prediction have been reported by few articles. This article aims to build the fatigue damage evolution model and to obtain the life property of TC18 through the low-cycle fatigue tests of standard fatigue samples. The static and low-cycle fatigue behaviors of TC18 titanium alloy were obtained, such as the stress-strain constitutive relationship, the cyclic stress-strain curve, the strain-life curve and fracture profiles. In

order to meet the requirements of engineering fatigue life evaluation for TC18, based on Manson-Coffin theory, the strain-life model was built and the low-cycle fatigue life curve was observed to investigate the life at certain confidence; on the other hand, combined with the damage mechanical theory, the damage gradual degradation process of the mechanical properties for TC18 titanium alloy with the increase of load cycles was described by the Lemaitre plastic damage model, and the fatigue damage accumulation parameters were determined based on test results.

LEMAITRE FATIGUE DAMAGE THEORY

Continuum damage mechanics is a branch of solid mechanics based on the continuum mechanical theory in recent decades. As introducing damage variables, it studies the law and mechanism of mechanical properties of structural materials from gradual degradation to failure with the loading cycles increased. Its advantages are thought that the mathematical form is relatively simpler and the physical meaning is clearer compared with traditional method. The LEMAITRE ductile damage model is commonly used to evaluate damage variations in elastic-plastic cases, and the initial damage induced by plastic deformation is described as following [3]:

$$\dot{D} = \left[\frac{\sigma_{eq}^2 R_v}{2ES(1-D)^2} \right]^m \dot{p} \quad (1)$$

Where σ_{eq} is the equivalent stress, MPa; \dot{p} is the cumulative plastic strain; S and m is the material parameters, determined by tests; E is Young's modulus, MPa; R_v is the function of stress triaxiality, defined as:

$$R_v = \frac{2}{3}(1+\nu) + \frac{(1-2\nu)}{3} \left(\frac{\sigma_H}{\sigma_{eq}} \right)^2 \quad (2)$$

Where ν is Poisson ratio, σ_H is the hydrostatic stress which is equal to $\sigma_{ij}e_i \otimes e_j / 3$.

When the sample is subjected to a single-axis load, formula (1) is integrated in a cycle, then we obtained:

$$\int_{1cycle} \dot{D} dt = \left[\frac{(\sigma_{max})^2}{2ES(1-D)^2} \right]^m \Delta p \quad (3)$$

where σ_{max} is the maximum stress amplitude in one loading cycle, MPa; Δp is the accumulated plastic strain in one loading cycle. For the strain-controlled fatigue loading case at constant amplitude, the damage value D is integrated from 0 to 1, the total fatigue life N is described as follows[4]:

$$N = \frac{1}{2(2m+1) \Delta \varepsilon_p} \left(\frac{2ES}{(\sigma_{max})^2} \right)^m \quad (4)$$

If the equation of cyclic stress-strain curve is written as follows [5]:

$$\sigma_{max} = k' \left(\frac{\Delta \varepsilon_p}{2} \right)^{n'} \quad (5)$$

Where k' , n' are material parameters, which will be determined by experimental results. Therefore the cycle number to failure at $\Delta\varepsilon_p$ is calculated by the following formula:

$$N = \frac{1}{2(2m+1)} \left(\frac{2^{1+2n'} ES}{k'^2} \right)^m (\Delta\varepsilon_p)^{-(1+2mn')} \quad (6)$$

Where m , S can be calibrated by the strain-life curve. If integrating formula (1) from 0 to D , the relation between damage value D , maximum stress amplitude σ_{\max} and loading cycle N is described as:

$$D = 1 - \left[1 - 2(2m+1) \left(\frac{\sigma_{\max}^2}{2ES} \right)^m \Delta\varepsilon_p N \right]^{\frac{1}{2m+1}} \quad (7)$$

Inserting formula (5) into formula (7), D can be calculated by the following formula:

$$D = 1 - \left[1 - 2(2m+1) \left(\frac{k'^2}{2^{2n'+1} ES} \right)^m \Delta\varepsilon_p^{2n'+1} N \right]^{\frac{1}{2m+1}} \quad (8)$$

Based on this relation, we can obtain the damage evolution rules with loading cycles increased if m , S , k' , n' , E are known, whereas these parameters will be determined by static and fatigue test results in view of formula (5) ~ (6).

STATIC PROPERTY OF TC18 TITANIUM ALLOY

The objective of this section is to obtain the Young's modulus(E), yield stress (σ_y) and Ultimate Tensile Strength (UTS) according the ASTM E8/E8M using both an extensometer and the measured cross-head displacement. The geometry size of test specimen is described in Figure 1. The static test was carried out by MTS extensometer with a gauge distance of 10 mm. The stress-strain curve of TC18 titanium alloy was obtained in view of [1]. When the test specimen was installed, the axis of the test machine was coincident with the test loading force line, so as to avoid the test specimen bearing other stress than the specified axial stress, and the test load was evenly distributed on the cross section. The installation morphology is shown in Figure 2. The tensile tests were performed on MTS machine at room temperature.

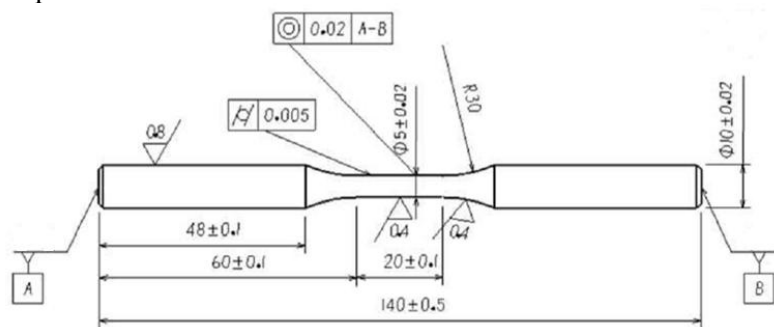


Figure 1: Sample geometry for static test and strain-controlled fatigue test



Figure 2: Installation morphology

The loading form was displacement controlled, and the loading rate was 1mm/min. All the 3 tensile tested samples failed after a considerable amount of necking in the gauge length of the samples. The tensile stress–strain curves are observed as shown in Figure 3 and Table 1 summarize the static tensile property of TC18 titanium alloy. The static performances measured on three samples are consistent. We will apply the mean values of the Young's modulus to determine the parameters of damage evolution model.

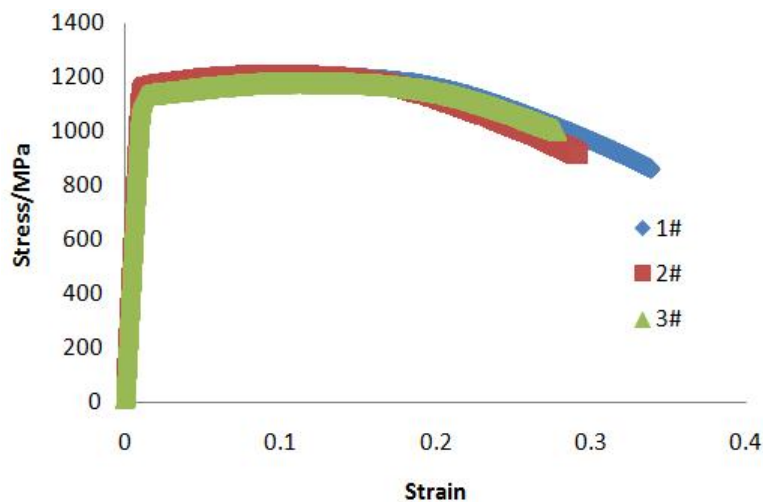


Figure 3: Stress-strain curves of TC18 titanium alloy

Table 1: Static test results of TC18 titanium alloy

<i>Sample Nums</i>	<i>E/MPa</i>	σ_y / <i>MPa</i>	<i>UTS/MPa</i>
1#	111462	1153	1206.5
2#	115397	1158	1211.2
3#	109698	1153	1185.8
Mean values	112186	1154.7	1201.2

FATIGUE PROPERTY OF TC18 TITANIUM ALLOY

Fatigue tests. The geometry of fatigue samples was coincident with the one of static samples. We chose six kinds of strain levels to obtain the fatigue lives of 27 samples for TC18 titanium alloy. According its static properties of tests, the strain-controlled fatigue test arrangement was shown in Table 2. Considering the small distribution of fatigue life at high strain loading, we relatively applied small number of samples to investigate its low-cycle fatigue property.

Table 2: Test arrangement of low-cycle fatigue tests

Strain level	1.28%	1.1%	1%	0.9%	0.8%	0.65%
Chosen Num	4	3	5	5	6	4

The fatigue tests were performed on MTS system at room temperature(15°C~18°C), and the control form was dominantly set as constant strain and the important inspection parameters. The test frequency was chosen between 0.3HZ and 1.0HZ. The stress ratio was -1 for all the cycles. We judge the structure in failure with the condition that the test samples was broken or the cyclic maximum tensile stress dropped to 70% of specified values.

We define $\Delta\varepsilon_t$ as the loading strain amplitude, Figure 4 is the curve of strain-fatigue lives obtained by tests. When $\Delta\varepsilon_t = 1.28\%$, the fatigue lives N_f of 4 samples are 404,445,458 and 436; When $\Delta\varepsilon_t = 0.65\%$, the fatigue lives N_f of 5 samples are respectively 24633,13278, 18594 and 26946. The dispersion of fatigue life becomes more and more obvious with the increase of loading strain amplitude. Figure 5 shows the stress-strain hysteresis loops at different strain levels. As shown in Figure 5, TC18 shows a certain softening tendency with the increase of fatigue cycles, which also can be illustrated in Figure 6. When the cyclic strain amplitude is 0.8%, stress-strain loop at one cycle is nearly in elastic state, resulting in the basic coincidence of its loading and unloading curves, and the area contained in the hysteresis loop is basically 0. For the loading strain amplitude is larger 0.8%, we can observe that the stress-strain curves tends to be steady when the loading cycles arrives at half of the fatigue lives. Consequently, the stress-strain loop at $N=N_f$ can be identified as the steady-state hysteresis loop.

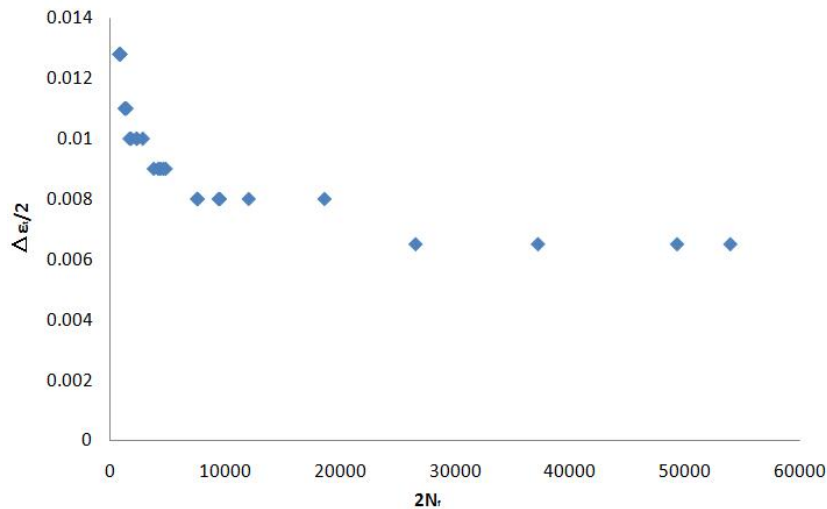


Figure 4: Strain-lives curves of TC18 titanium alloy

Parameters Determination of Mason-Coffin model. The cyclic stress at the steady state can be determined by the cyclic stress-strain responses of test results, and the cyclic stress-strain behaviour is obtained as shown in Figure 6. Comparing the material's monotonic and cyclic stress-strain curves, the cyclic behaviour clearly lies below the monotonic behaviour, thus we can define the TC18 titanium alloy is cyclically softening. In view of plastic mechanism theory, we define it based on the cyclic strength coefficient (k') and strain hardening exponent (n'), and the cyclic stress-strain relation can be characterized by the Ramberg-Osgood type model as follows:

$$\frac{\Delta\varepsilon_t}{2} = \frac{\Delta\varepsilon_e}{2} + \frac{\Delta\varepsilon_p}{2} = \frac{\Delta\sigma}{E} + \left(\frac{\Delta\sigma}{2k'} \right)^{1/n'} \quad (9)$$

We can obtain the elastic and plastic components based on formula(9).

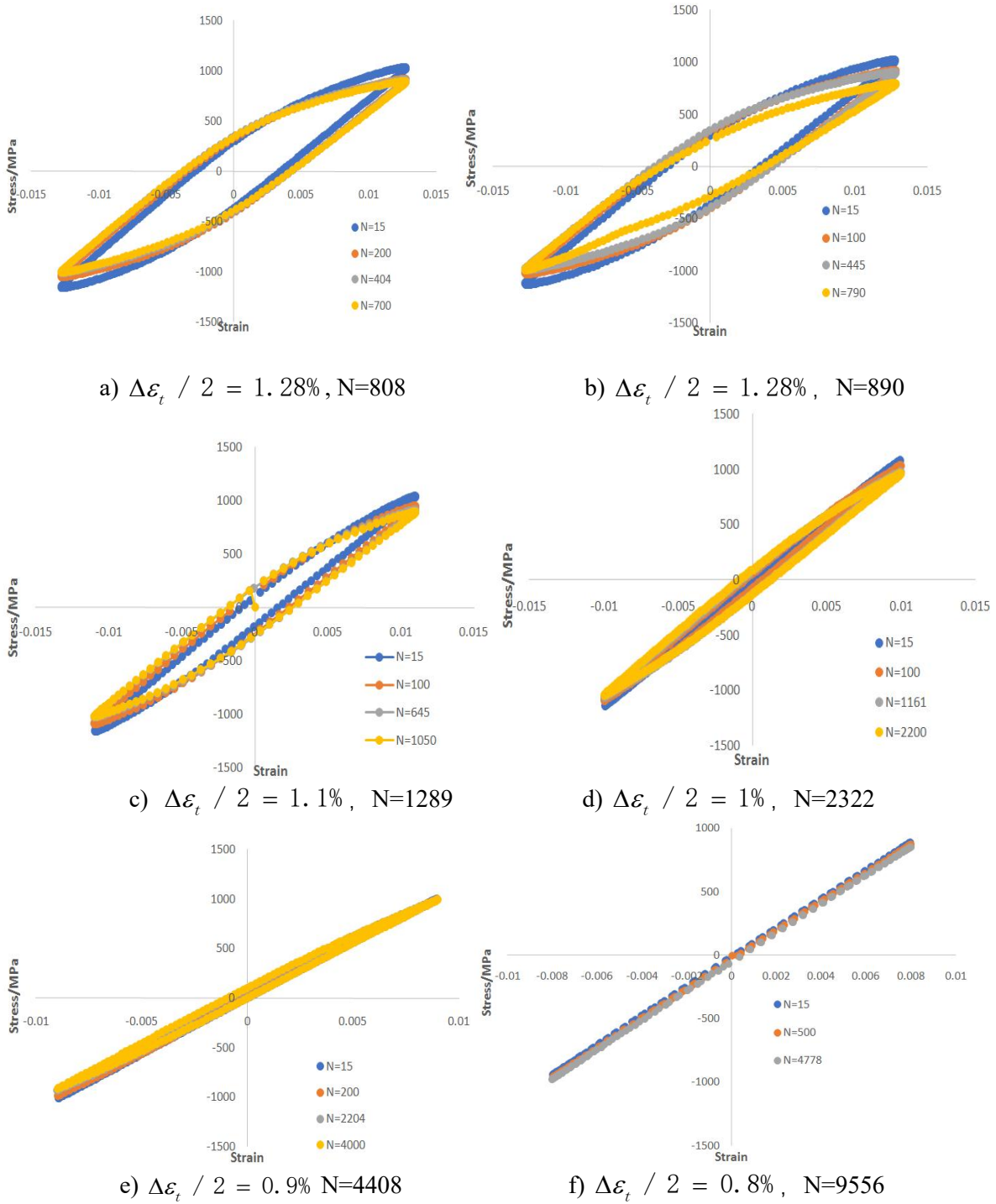


Figure 5: Stress-strain hysteresis loops of TC18 titanium alloy at different strains

And the plastic strain deformation behaviour can be written as follows:

$$\frac{\Delta\varepsilon_p}{2} = \left(\frac{\Delta\sigma}{2k'} \right)^{1/n'} \quad (10)$$

In view of the test results of the steady-state cyclic stress, loading strain amplitude and average Young's modulus E , we can determine the plastic strain $\Delta\varepsilon_p$ by formula (10). The corresponding

unknown parameters k' and n' were fitted as $k' = 944.4$, $n' = -0.02625$ by the least squares method. The fitted curve is shown in Figure 6.

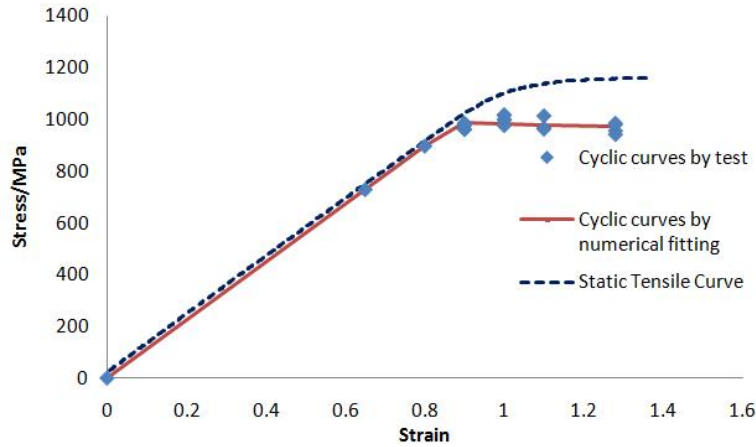


Figure 6: Cyclic true stress-true strain curves

The Manson-Coffin model is applied to characterize the relation between the loading strain amplitude $\Delta\varepsilon_t$ and N as follows:

$$\frac{\Delta\varepsilon_t}{2} = \frac{\sigma_f'}{E} (2N_f)^b + \varepsilon_f' (2N_f)^c \quad (11)$$

where σ_f' is the fatigue strength coefficient, ε_f' is fatigue ductility coefficient, b and c are the corresponding index. Those unknown parameters can be determined by the numerical fitting of strain-fatigue life curve. Therefore, we obtain the strain-fatigue live prediction model as following:

$$\frac{\Delta\varepsilon_t}{2} = \frac{3836.76}{112186} (2N_f)^{-0.1613} + 3.538e-6 (2N_f)^{0.4541} \quad (12)$$

MICROGRAPHS OF THE FAILURE SURFACES OF TC18 TITANIUM ALLOY

Failure Analysis Arrangement. 3 samples were chosen to analyse the fracture surface of different loading types, the details of samples are listed in Table 4. The fracture surfaces were investigated at higher magnification to study the nature of the fracture by TESCAN Scanning Electron Microscope.

Table 3: Samples for Failue analysis

Nums	FA-1	FA-2	FA-7
Cyclic Strain	Static	1.28%	0.65%
Fatigue life	tensile test	872	26556

Regarding the fracture surface of static tensile testing sample, the region of the crack initiation, crack growth and shear are investigated in Figure 7. Crack initiates in the central zone of fracture surfaces, and it propagates along the radial direction, and finally fractures as the shearing mode at the edge of the sample. The fracture morphology is shown in figure 7(b) and 7(c), the whole surface is characterized of typical dimple fracture.

Figure 8 is the crack initiation zone, crack propagation zone and shear lip zone of the sample FA-2. It was loaded at constant amplitude $\Delta\varepsilon_t / 2 = 1.28\%$, and the fatigue life was 872 cycles. The figure shows that the crack initiates at the edge of the fracture surface, then propagates to the other side, finally failures at the edge. There are two zones of propagation,

the zone I is quasi-cleavage feature, and the zone II is a mix of quasi-cleavage and dimple fracture, yet mainly in quasi-cleavage feature and the shear lip zone is dimple feature.

Figure 9 is the SEM fractography of sample loaded at $\Delta\epsilon_f / 2 = 0.65\%$, its fatigue life was 26556 cycles. The fracture mode is mainly consistent with the one of sample FA-2, yet the crack propagation zone I and II are the quasi-cleavage fracture, and fatigue striations can be clearly presented in zone I, zone III is dimple fracture.

The following results can be obtained from the fractography of strain-controlled fatigue tests for TC18 titanium alloy:

- 1) The crack initiation locations of static testing sample and fatigue testing sample are different. The static one initiates at the central zone, yet the fatigue one initiates at the edge zone.
- 2) The static tensile fracture is characterized as full-dimple feature (tensile dimple or shear dimple), while the fatigue samples initiate as the quasi-cleavage feature, and propagate as the quasi-cleavage feature or a mix of quasi-cleavage and dimple features.

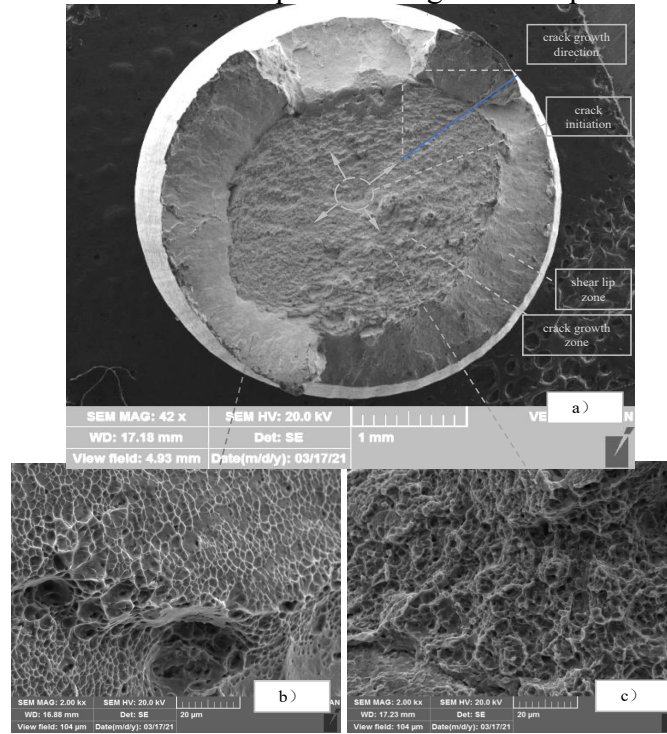


Figure 7: SEM fractography of static tensile sample a) macroscopic fracture, b) shearing dimple, c) tensile dimple

DAMAGE EVOLUTION ASSESSMENT OF TC18 TITANIUM ALLOY

We built the damage mechanical model as formula (8) to describe the damage evolution rules with the loading cycles increased at certain loading strain. The parameters m , S will be determined by test results of the plastic strain-fatigue life values. Based on formula (6), they can be numerically fitted by least-square method in Figure 10. We obtained $m=7.955$, $S=9.3242$ when $k'=944.4$, $n' = -0.02625$ and $E=112186$ MPa. Consequently, the relation between damage evolution value and fatigue life is described as:

$$D = 1 - (1 - 0.051229\Delta\epsilon_p^{0.582349}N)^{0.059135} \quad (13)$$

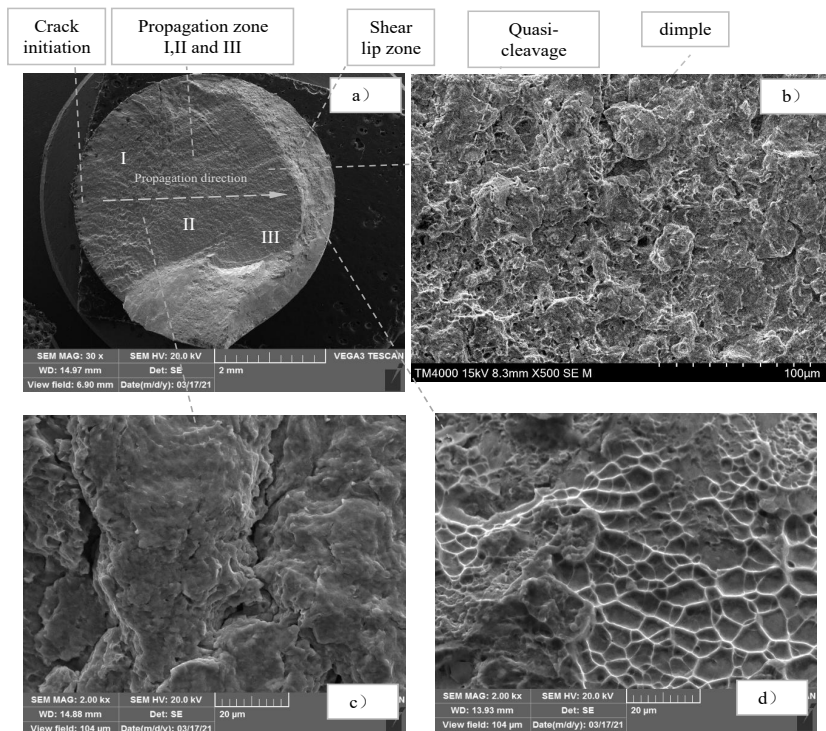


Figure 8 : SEM fractography of low-cycle fatigue sample at $\Delta\epsilon_t / 2 = 1.28\%$, $N/2=872$ a) macroscopic fracture, b)quasi-cleavage+dimple, c) quasi-cleavage d) shearing dimple

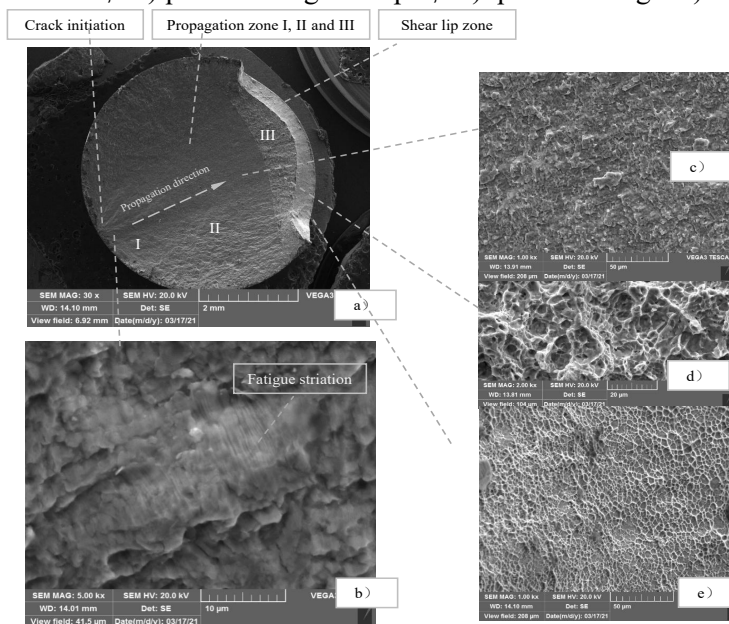


Figure 9: SEM fracture morphology of fatigue sample at $\Delta\epsilon_t / 2 = 0.65\%$, $N/2=26556$ a) macroscopic fracture, b) quasi-cleavage, c) quasi-cleavage d) dimple e) shear dimple

If the plastic strain loading is known, we can obtain the damage evolution rules of the samples subjected to the strain-controlled fatigue loading. Figure 11 is the evolution rules at different plastic strain amplitude. As shown in Figure 11, the damage slowly evolves when D is smaller than 0.1, then the propagation rate of fatigue damage gradually increases until the sample failures ($D=1$). When $\Delta\epsilon_p$ is larger, the fatigue life is smaller. The same damage needs more loading cycles if $\Delta\epsilon_p$ is smaller.

To be noted, in view of Finite element method, we can predict the fatigue damage evolution and fatigue life of structures with the irregular geometry or subjected to complicated random loading based on formula (16) and elastic-plastic mechanical theory.

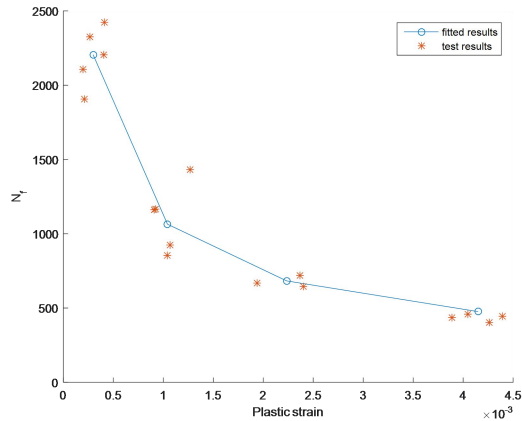


Figure 10: Plastic strain- fatigue life fitted results based on formula (6)

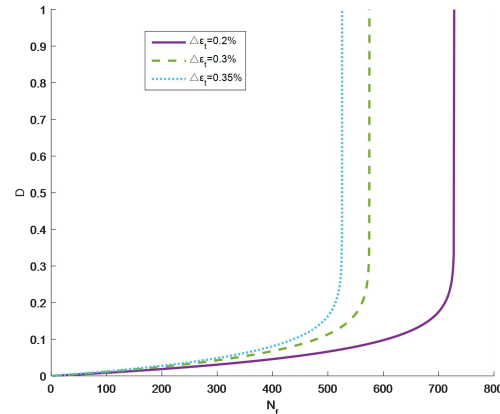


Figure 11: Damage evolution rules with N_f increased at different plastic strain amplitude

CONCLUSION

The low-cycle fatigue property of TC18 titanium alloy was investigated in this paper and the following conclusions can be obtained:

- 1) Firstly, the damage evolution model of structures subjected to single-axis load was derived based on Lemaitre fatigue damage mechanical theory.
- 2) To determine the unknown parameters in the damage model, we studied and obtained the static strength, cyclic stress-strain property and strain-fatigue life curves by static and fatigue tests of the standard sample, and the corresponding predicted models were reserved by numerical fitting. The research indicated that TC18 titanium alloy was material cyclically softening, and the damage evolution rules at different plastic strain loading were presented to predict the fatigue damage state of structures under certain loading cycles.
- 3) Fracture morphologies of TC18 titanium alloy were analyzed by SEM, and the results showed that the crack initiation locations of static testing sample and fatigue testing sample were different, which the static one initiated at the central zone, and the fatigue one initiated at the edge zone.

REFERENCES

- [1] SUN Shuyu, LV Weijie (2016), *Rare Metal Materials and Engineering*, Vol.45,n.5,p.1138-1141.
- [2] QU F.S., ZHOU Y.H., ZHANG Z.H et al(2015). *Material & Design*, vol.69,p.153-162.
- [3] Lemaitre J., Desmorat R (2005),. In: *Engineering damage mechanics: ductile, creep, fatigue and brittle failures*, Springer:2005.p.188-189.
- [4] ZHAN Zhixin, HU Weiping, SHEN Fei et al.(2017). *International Journal of Fatigue*, vol.96,p.208-223.
- [5] ASTM E606-04: Standard practice for strain-controlled fatigue testing.
- [6] B/Z112-86: Statistical analysis of material fatigue testing data.